ELSEVIER

Polymer 41 (2000) 3561–3580

polymer

Synthesis and characterization of poly(copolyethers-*block*-polyamides) II. Characterization and properties of the multiblock copolymers

A. Boulares, M. Tessier, E. Maréchal*

Laboratoire de Synthèse Macromoléculaire (CNRS, UMR 7610 Chimie des Polymères), Université Pierre et Marie Curie, Case 184-4, Place Jussieu, 75252 Paris Cedex 05, France

Received 7 April 1999; received in revised form 21 July 1999; accepted 28 July 1999

Abstract

Multiblock copolymers were synthesized from an α,ω-dicarboxy-oligododecanamide (PA12dC; $\bar{M}_n = 2095$) and various α,ω-dihydroxy-polyethers ($\bar{M}_n = 1000–2000$), especially, as copolyethers containing both polyoxyethylene and polyoxypropylene blocks. The polycondensation reaction was carried out in bulk at high temperature in the presence of $Zr(OBu)_4$ as catalyst. A kinetic study permitted one to compare the reactivity of the different oligoethers used with respect to PA12dC. The thermal properties, the structure and morphology of these poly(polyethers-*block*-polyamides) were characterized by DSC, TGA, DMA and solid-state ^{13}C NMR. DSC and DMA results show that the multiblock copolymers based on copolyethers exhibit a very high degree of phase separation and these soft blocks do not crystallize, whatever their length and composition. NMR results reveal that the crystalline polyamide phase adopts a structure (γ-form) similar to that of the oligoamide precursor.

Keywords: Poly(polyethers-*block*-polyamides); Copolyethers; Carboxy end group

1. Introduction

Poly(polyethers-*block*-polyamides) (PEBAs) is a combination of a polyamide as a hard block and a polyether as a soft block; these have been widely studied as thermoplastic elastomer [1–8].

Polyamide-11, polyamide-12 and polyamide-6 are the most widely used polyamides, as the hard blocks. Polyoxytetramethylene (POTM), polyoxyethylene (POE) and polyoxypropylene (POP) are often chosen as the polyether blocks.

The microphase separation, the crystallinity of each phase, the hydrophobicity and the properties of the resulting multiblock copolymers, depend on the nature and the molar mass of hard and soft blocks [4,9–11].

Some of these PEBAs are commercialized by Elf Atochem and by Hüls under the trade name of PEBAX® and VESTAMID®, respectively. However, changes in the morphology of the polyether blocks are observed when the materials are used at room temperature. With semicrystalline polyethers (POTM or POE), the melting temperature of the corresponding segments leads to a variation of storage modulus harmful to the use of material in this temperature range. Polyoxypropylene could be selected, as it does not crystallize in these conditions; however it raises important problems because the resulting PEBA is obtained by polycondensation of the α,ω-dicarboxy-polyamide with the α,ω-dihydroxy-polyoxypropylene, and the hydroxy end groups of the telechelic oligoether are mainly secondary. The low reactivity of these end groups prevents the formation of high molar mass multiblock coplolymers. Moreover, a degradation of these units is observed during the polycondensation.

These drawbacks could be overcome by the use of amorphous or semicrystalline (with a low degree of crystallinity) telechelic copolyethers; such samples are commercially available.

This article is relative to new PEBAs based on polyamide-12 and block copolyethers of ethylene oxide and propylene oxide: they were obtained by polycondensation of an α,ω-dicarboxy-oligododecanamide (PA12dC; $\bar{M}_n = 2095$) with various α,ω-dihydroxy triblock copolyethers such as polyoxyethylene-*block*-polyoxypropylene-*block*-polyoxyethylene (POE/POP/POE dOH; $\bar{M}_n = 1000–2000$). A kinetic study of the polycondensation and some properties of the resulting multiblock copolymers compared with those of PEBAX® are described.

* Corresponding author. Fax: +33-1-4427-7054.

0032-3861/00/$ - see front matter
PII: S0032-3861(99)00526-1

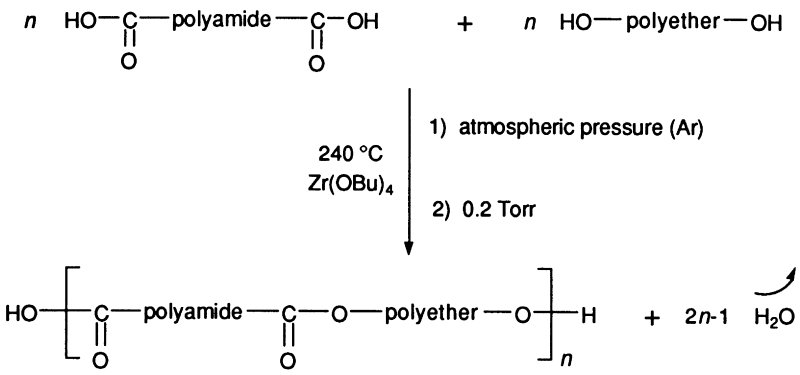

Scheme 1.

2. Experimental

2.1. Materials

The chemicals α,ω-dihydroxy-oligooxytetramethylene (POTMdOH), oligooxyethylene (POEdOH) and oligooxypropylene (POPdOH) were provided by BASF. Synperonic® and Pluronic® copolyethers were provided by ICI and by BASF, respectively. α,ω-Dicarboxy-oligododecanamide (PA12dC) was provided by Elf Atochem. The oligomers were used without further purification.

2.2. Polycondensations

Kinetic study. The general procedure is described as follows: PA12dC and α,ω-dihydroxy-polyethers in stoichiometric molar ratio were placed in a 100 ml glass reactor equipped with an argon inlet and outlet, a central mechanical stirrer and a condenser. The reactor was placed in an oil bath at the desired temperature. When thermal equilibrium was reached (ca. 15 min), for the non-catalyzed reactions, samples were taken at suitable time intervals; for the catalyzed reactions, $Zr(OBu)_4$ (in CH_2Cl_2 solution) was introduced into the mixture with the help of a hypodermic syringe, and the resulting mixture was stirred for 1 min, then samples were taken as in the case of non-catalyzed reactions.

Synthesis of high molar mass block copolymers. A stoichiometric amount of PA12dC and α,ω-dihydroxy-polyether were polycondensed in bulk, in the presence of $Zr(OBu)_4$ (1.5 mmol kg^{-1}). In a first step, the reaction was carried out at 240°C, under argon atmosphere, for 2 h; the second step was conducted under vacuum (0.3 torr) for 3 h.

2.3. Measurements

^1H NMR spectra were recorded in TFA/$CDCl_3$ (1/4 v/v) on a Bruker AM 500 spectrometer. The chemical shifts were referenced to residual $CHCl_3$ at 7.26 ppm.

Solid-state ^{13}C NMR spectra were recorded on Bruker MSL 200 or MSL 300 spectrometers. The chemical shifts were referenced to adamantane (29.5 ppm). In most cases, a 1 ms contact time and a 5 s recycle delay were used. The different peaks were deconvoluted using a computer program for simulating NMR line shapes in solids as combination of Gaussian and/or Lorentzian line shapes.

Size exclusion chromatography (SEC) was performed in benzyl alcohol at 130°C (1 ml min^{-1}) in Elf Atochem laboratory with a Waters equipment: U6K injector, 510 pump, 410 Differential refractometer and a PL-Gel column set (60 cm mixed and 30 cm 500 Å). The system was calibrated with polyoxytetramethylene standards.

The dynamic mechanical measurements were performed on compression-molded specimens and were carried out in Elf Atochem laboratory on a Rheometrics RMS 800 apparatus equipped with a torsional pendulum. The temperature range between −120 and 160°C was scanned at a heating rate of 5°C/min and at a constant frequency of 10 Hz.

Differential scanning calorimetry (DSC) was carried out on a DSC 2010 CE TA Instruments apparatus equipped with the liquid nitrogen cooling LNCA accessory at a cooling and heating rate of 20°C/min, or on a Perkin–Elmer DSC 7 apparatus at a heating rate of 20°C/min under nitrogen atmosphere. Crystalline melt temperatures (T_m) were taken as the minima of the melting endotherms and the glass transition temperatures (T_g) were obtained at the inflection point from the second heating run.

Thermogravimetric analysis (TGA) was carried out on a DuPont Instruments 9900 Thermal Analyzer system equipped with a 951 Thermogravimetric Analyzer at a heating rate of 10°C/min under nitrogen atmosphere.

X-ray diffraction experiment was performed on oligoamide-12 (PA12dC) powder in Elf Atochem laboratory using a Rigaru RU-200 generator. The instrument was equipped with a CuKα radiation ($\lambda = 1.54$) X-ray source operating at 40 kV and 30 mA.

Titration of carboxy end groups was carried out under nitrogen atmosphere using a Mettler DL40RC automatic potentiometric titrator. Samples were previously dissolved in boiling benzyl alcohol. After cooling at room temperature,

Table 1
Number-average molar mass ($\bar{M}_n$), OE/OP ratio of the numbers of OE and OP units and percentages of primary (% *pri*-OH) and secondary (% *sec*-OH) hydroxy end groups of initial oligomers

Sample	$\bar{M}_n$ [a]	OE/OP[a]	% *pri*-OH[a]	% *sec*-OH[a]
PA12dC	2095[b]			
POTMdOH	1000		100	
POEdOH	1050		100	
POPdOH	880			100
Synperonic®L-31	1090	0.25	50	50
Synperonic®L-35	1920	1.26	90	10
Synperonic®L-42	1570	0.26	75	25
Synperonic®L-61	1950	0.23	60	40
Pluronic®3100	1095	0.16	35	65
Pluronic®4300	1925	0.65	80	20
Pluronic®6100	1740	0.14	45	55

[a] Determined by ^{1}H NMR.
[b] Determined by end group titration.

the resulting solution was titrated with KOH/ethanol solution. A blank titration was carried out.

Water content in polyether samples was determined by the Karl Fischer titration.

Inherent viscosities were measured from *m*-cresol solutions (0.5 g dl^{-1}) by using a Schott automatic viscosimeter with a Ubbelhode 538-23 capillary microviscosimeter in a constant temperature water bath (Schott CT 1450) kept at 20°C.

3. Results and discussion

The polycondensations were performed according to the same process, in bulk at high temperature and in the presence of tetrabutoxyzirconium ($Zr(OBu)_4$) as catalyst. The reagents (i.e. PA12dC and α,ω-dihydroxy-polyether) were introduced in the reactor in a stoichiometric molar ratio. The general procedure is described in Scheme 1. The characteristics of the initial oligomers were already described in previous studies [12,13]; they are summarized in Table 1: ($\bar{M}_n$), OE/OP (where OE and OP are the numbers of oxyethylene and oxypropylene units, respectively) and the molar percentages of primary and secondary hydroxy end groups. PA12dC used throughout the study presents two structures:

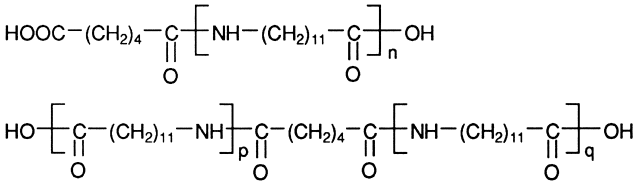

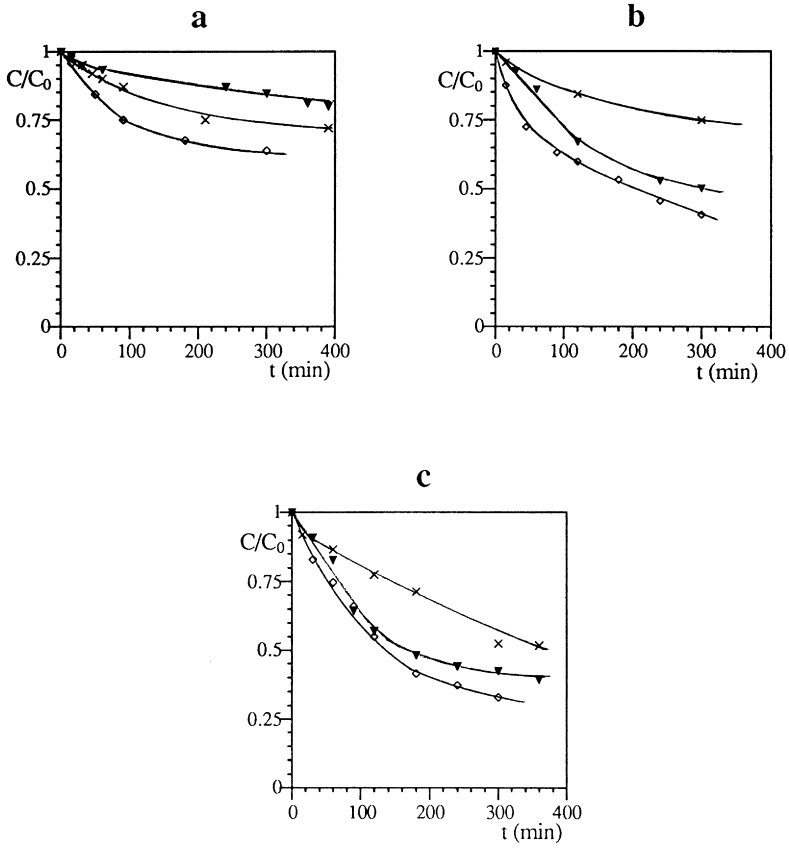

Fig. 1. Variation of C/C_0 versus time. Polyesterification of PA12dC with: ◇—POTMdOH; ▼—POEdOH; × —POPdOH; at (a) 200°C; (b) 220°C; (c) 240°C.

Table 2
Water content in the oligomer precursors (% in mass)

Sample	H_2O (%)
PA12dC	0.35
POTMdOH	0.32
POEdOH	0.62
POPdOH	0.50
Synperonic®L-31	0.17
Synperonic®L-35	0.22
Pluronic®6100	0.25

3.1. Polyesterification of α,ω-dicarboxy-oligododecanamide with several α,ω-dihydroxy-oligoethers

The kinetics and mechanisms of esterification reactions catalyzed by various organometallic derivatives have extensively been investigated [14,15].

In this study, the polyesterification reaction was studied at three temperatures (200, 220, 240°C) in the absence and in the presence of $Zr(OBu)_4$ (1.5 or 3 mmol kg^{-1} of reactive mixture). Kinetic experiments were carried out only under atmospheric pressure (see experimental part). The reaction was followed by chemical titration of the carboxy end group concentration (C, eq g^{-1}) at different reaction times t (min).

3.1.1. Polycondensation of POTMdOH, POEdOH and POPdOH with PA12dC

3.1.1.1. Non-catalyzed polycondensation The variation of C/C_0 versus time are reported in Fig. 1. C_0 and C are carboxy end group concentrations at time $t = 0$ and at time t, respectively. Whatever the polyether, the concentration of reacted carboxy groups increases with increasing reaction temperature (200, 220, 240°C).

At 220 and 240°C, POTMdOH is slightly more reactive than POEdOH whereas POPdOH reactivity is far lower than that of the two others. These results are consistent with the nature of hydroxy end groups: POPdOH has only secondary hydroxy end groups which are less reactive than primary ones.

At 200°C, the reactivity increases is as follows: POEdOH < POPdOH < POTMdOH. Esterification rate depends on the water content in the reactive medium; water is already present in the mixture before reaction takes place (Table 2) and is released by the polycondensation. POEdOH is particularly hygroscopic and it contains

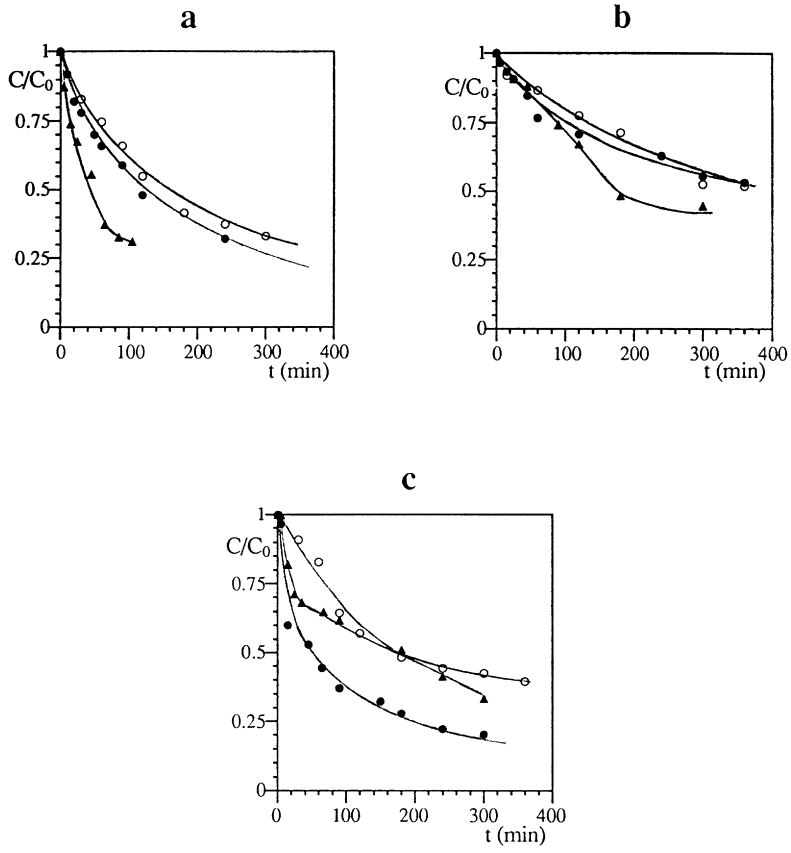

Fig. 2. Variation of C/C_0 versus time. Polyesterification of PA12dC at 240°C with: (a) POTMdOH: ○—without catalyst; ●—with 1.5 mmol kg^{-1} of $Zr(OBu)_4$; ▲—with 3 mmol kg^{-1} of $Zr(OBu)_4$; (b) POPdOH: ○—without catalyst; ●—with 1.5 mmol kg^{-1} of $Zr(OBu)_4$; ▲—with 3 mmol kg^{-1} of $Zr(OBu)_4$; (c) POEdOH: ○—without catalyst; ●—with 1.5 mmol kg^{-1} of $Zr(OBu)_4$; ▲—with 3 mmol kg^{-1} of $Zr(OBu)_4$.

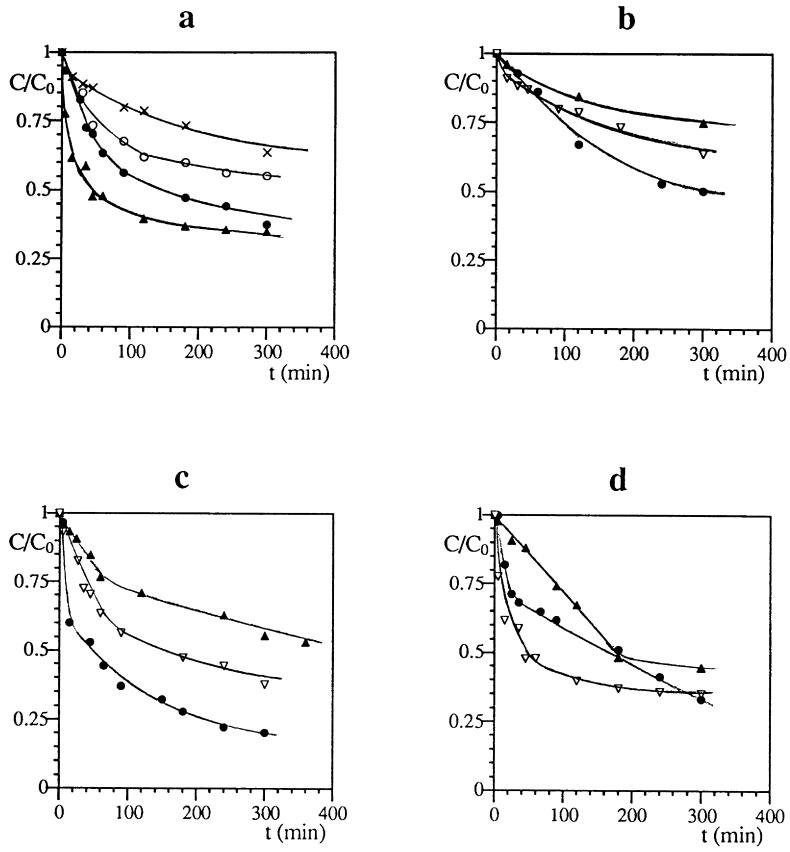

Fig. 3. Variation of C/C_0 versus time. Polyesterification of PA12dC: (a) with Synperonic®L-31: ×—at 220°C without catalyst; ○—at 240°C without catalyst; ●—at 240°C with 1.5 mmol kg^{-1} of $Zr(OBu)_4$; ▲—at 240°C with 3 mmol kg^{-1} of $Zr(OBu)_4$; (b) at 220°C with: ▲—POPdOH; ▽—Synperonic®L-31; ●—POEdOH; (c) at 240°C in the presence of 1.5 mmol kg^{-1} of $Zr(OBu)_4$ with: ▲—POPdOH; ▽—Synperonic®L-31; ●—POEdOH; (d) at 240°C in the presence of 3 mmol kg^{-1} of $Zr(OBu)_4$ with: ▲—POPdOH; ▽—Synperonic®L-31; ●—POEdOH.

more water than the other two oligomers, which explains its low polyesterification rate value at 200°C, as water is not completely eliminated from the reaction medium at this temperature.

3.1.1.2. $Zr(OBu)_4$-catalyzed polycondensation When the polycondensation is carried out in the presence of $Zr(OBu)_4$, it is more difficult to analyze the influence of experimental conditions on the results. The behavior of the catalyst depends on several parameters, particularly its concentration, water content and medium polarity. Laporte et al. [15] reported the study of the influence of these parameters on $Zr(OBu)_4$-catalyzed esterifications and polyesterifications.

Independently of its interaction with reactive end groups (carboxy and hydroxy groups), $Zr(OBu)_4$ yields species of different structure as free molecules, clusters, aggregates and chelated forms.

The association degree of the clusters depends on medium polarity and on temperature. In dilute solutions, mainly dimers and trimers are formed. Zirconium coordination number reaches six or it can even be higher.

The formation of aggregates arises from the reaction of the catalyst with water: butoxy groups are partly replaced by hydroxy ones and the latter condense leading to ether bridges (Zr–O–Zr). Zirconium atom is chelated by the oxygen atoms of polyether chains.

The contribution of these parameters makes it impossible to determine the effective concentration of catalytic centres. Only free molecules and the active sites on the surface of aggregates have a catalytic effect.

The behavior of POTMdOH when it is polycondensed at 240°C is shown in Fig. 2a. Esterification rate and especially the initial rate, increases with increasing catalyst concentration.

Addition of catalyst (1.5 or 3 mmol kg^{-1}) to POPdOH/PA12dC system leads only to a low increase of initial reaction rate (Fig. 2b). When $Zr(OBu)_4$ concentration is 3 mmol kg^{-1}, the plot shows a slight autoacceleration (particularly perceptible when reaction time is 120 min). This phenomenon was already observed by Laporte et al. [15] in the case of the $Zr(OBu)_4$-catalyzed reaction between 11-dodecylaminoundecanoic acid and 2-tridecanol carried out under atmospheric pressure at 180–190°C with high catalyst concentration ($\geq$2.9 mmol kg^{-1}). These authors assumed that this autoacceleration arises from the cleavage of catalyst clusters or aggregates, in the presence of esterification water and carboxy groups, increasing the reactive catalytic site number.

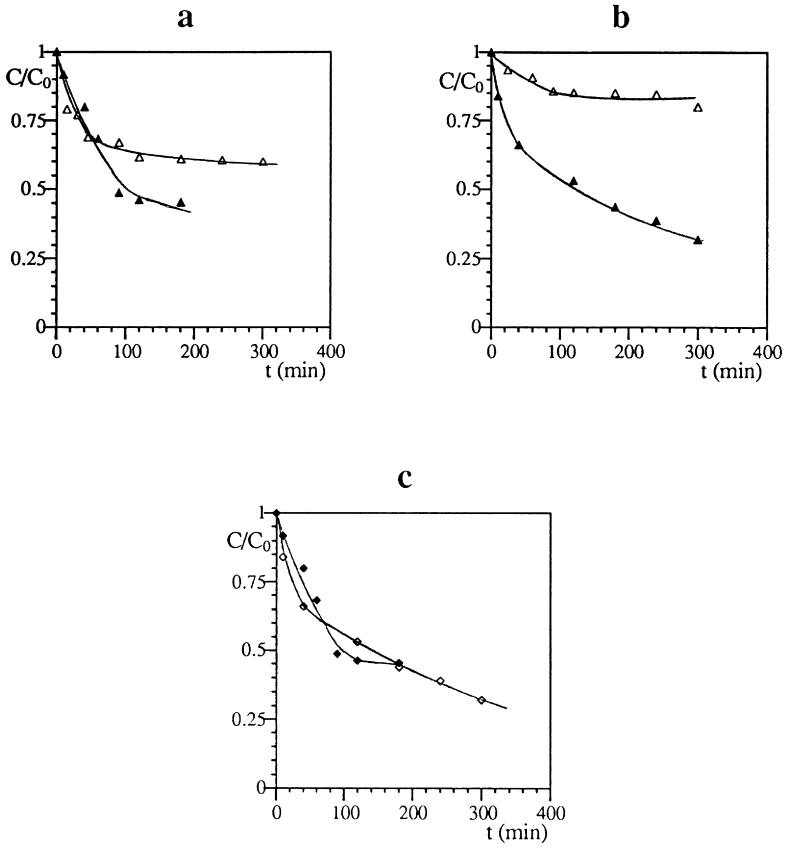

Fig. 4. Variation of C/C_0 versus time. Polyesterification of PA12dC at 240°C: (a) with Synperonic®L-35: △—without catalyst; ▼—with 3 mmol kg^{-1} of $Zr(OBu)_4$; (b) with Pluronic®6100: △—without catalyst; ▲—with 3 mmol kg^{-1} of $Zr(OBu)_4$; (c) in the presence of 3 mmol kg^{-1} of $Zr(OBu)_4$ with: ◆—Synperonic®L-35; ◇—Pluronic®6100.

The addition of catalyst to POEdOH/PA12dC system (Fig. 2c) drastically increases initial reaction rate. However, the reaction slows down after 30 min when catalyst concentration is 3 mmol kg^{-1}. Laporte et al. [15] observed that catalytic efficiency is not proportional to catalyst concentration when the 11-dodecylaminoundecanoic acid/α-dodecyl-ω-hydroxy-polyoxyethylene ($\bar{M}_n = 350$) system is carried out under atmospheric pressure, at 180 or 240°C, and with $[Zr(OBu)_4] \leq 6.7$ mmol kg^{-1}; this results from the condensation of catalyst molecules and from the chelation of zirconium atoms by polyoxyethylene oxygen atoms.

In view of the preceding remarks, it is difficult to compare the behavior of the different $Zr(OBu)_4$-catalyzed systems; the only significant observation is that POPdOH is the least reactive of the three oligoethers whatever the experimental conditions.

3.1.2. Polycondensation of Synperonic®L-31, Synperonic®L-35 and Pluronic®6100 with PA12dC

The results relative to the polyesterification of Synperonic®L-31 with PA12dC carried out under atmospheric pressure in the absence of catalyst (at 220 and 240°C) or in the presence of $Zr(OBu)_4$ at 240°C are reported in Fig. 3a.

As expected, polyesterification rate increases with increasing temperature and catalyst concentration. In the absence of catalyst at 220°C (Fig. 3b), or in the presence of $Zr(OBu)_4$ (1.5 mmol kg^{-1}) at 240°C (Fig. 3c) this system exhibits a reaction rate intermediate between those of POPdOH/PA12dC and POEdOH/PA12dC systems (Synperonic®L-31 has a molar mass close to those of POEdOH and POPdOH). This result is consistent with the nature of Synperonic®L-31 end groups: equal amount of primary and secondary alcohol functions instead of two primary hydroxy groups for POEdOH and two secondary hydroxy groups for POPdOH. However, at 240°C with 3 mmol kg^{-1} of $Zr(OBu)_4$ (Fig. 3d), the Synperonic®L-31/PA12dC system gives the highest initial reaction rate; in the same experimental conditions, we observed that POEdOH exhibits a particular behavior, but the Synperonic®L-31 structure contains few oxyethylene units (OE/OP = 0.25) which should not modify the kinetics.

The kinetic plots relative to Synperonic®L-35/PA12dC and Pluronic®6100/PA12dC systems are reported in Figs. 4a and b, respectively; for these two systems carried out at 240°C under atmospheric pressure (the two initial copolyethers have similar molar masses), the conversion increases when $Zr(OBu)_4$ is added. Without catalyst, the reaction rate relative to Pluronic®6100/PA12dC system is much lower than that of the other system; this is due to a significant content of secondary hydroxy end groups in

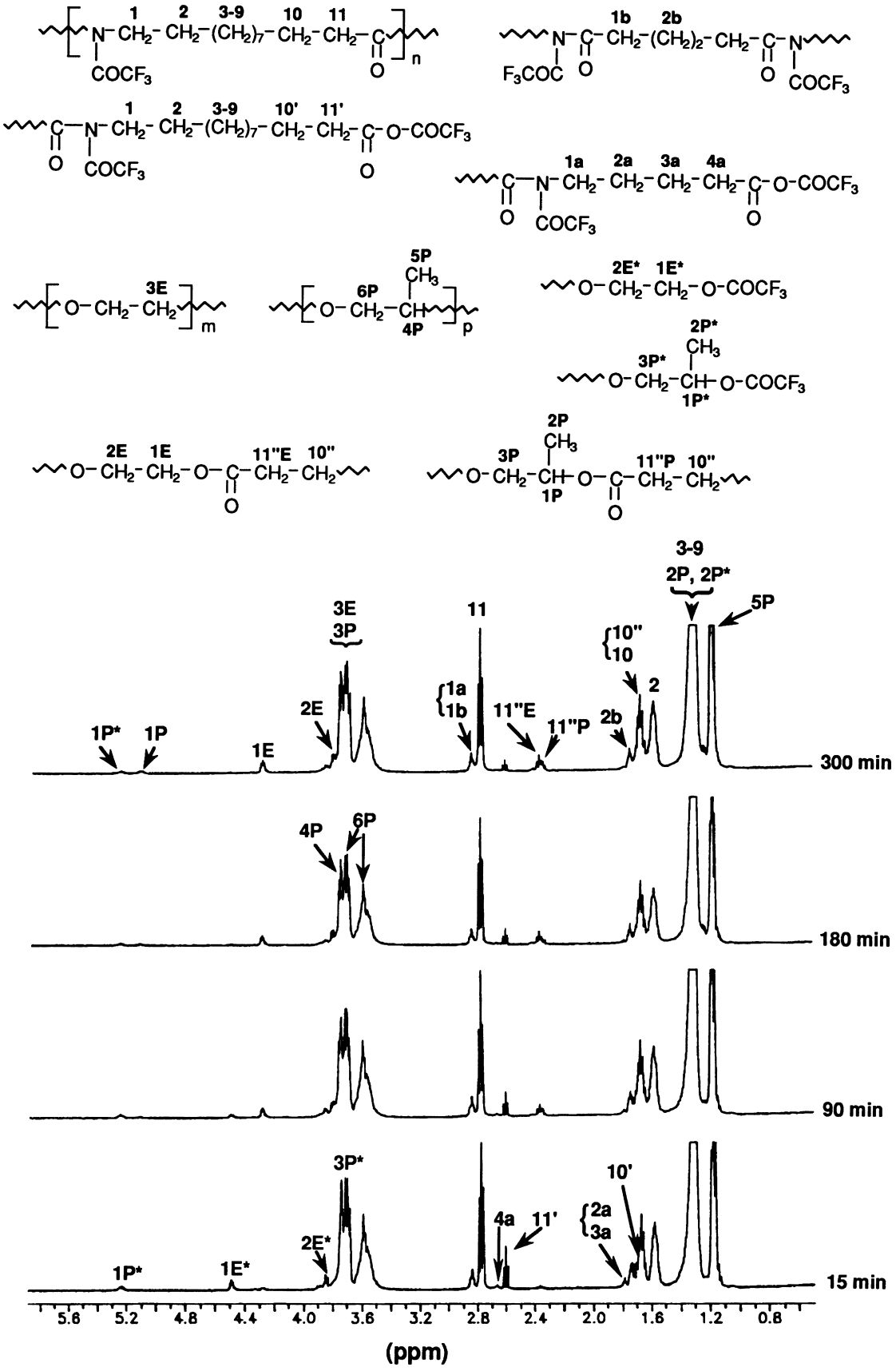

Fig. 5. ^{1}H NMR spectra of the Synperonic®L-31/PA12dC system (240°C; $[Zr(OBu)_4] = 1.5$ mmol kg^{-1}) at different reaction times; ($CDCl_3$/TFA).

Table 3
Inherent viscosity η_{inh}, number-average molar mass $\bar{M}_n$, polydispersity index I_p of PEBAs

Sample	η_{inh} (dl.g^{-1})	$\bar{M}_n$	I_p
PEBAX®(2000/2000)	1.41	16820	2.2
PEBAX®(2000/1000)	1.49	19720	2.3
PA-POTM(2095/1000)	1.37	9270	3.6
PA-POE(2095/1050)	0.80	6510	3.5
PA-POP(2095/880)	0.85	6260	4.1
PA-SL31(2095/1090)	0.99	10210	3.3
PA-SL35(2095/1920)	1.27	–	–
PA-SL42(2095/1570)	0.80	–	–
PA-SL61(2095/1950)	0.98	7190	4.5
PA-P3100(2095/1095)	1.05	10440	4.9
PA-P4300(2095/1925)	0.75	16820	2.3
PA-P6100(2095/1740)	Insoluble	–	–

Pluronic®6100 (45% againts 10% for Synperonic®L-35). When catalyst concentration is 3 mmol kg^{-1}, both systems have the same kinetic behavior (Fig. 4c) which is rather surprising. The reactivity of Synperonic®L-35 is lower than expected; however its OE content is relatively high (OE/OP = 1.26) which reduces the efficiency of the catalyst.

The kinetics of the Synperonic®L-31/PA12dC system (240°C; [Zr(OBu)$_4$]= 1.5 mmol kg^{-1}) was also followed by ^{1}H NMR; the corresponding samples were solubilized in a mixture of $CDCl_3$/trifluoroacetic anhydride (TFA) which was already used with initial precursors [12,13]. TFA reacts with amide, amine, hydroxy and carboxy groups. The ^{1}H NMR spectra recorded at different reaction times (Fig. 5) show on the one hand the decrease of signals relative to methylene protons in α-position of carboxy end groups ($\delta = 2.60$ ppm) and to methylene and methine protons in α-position of trifluoroacetylated hydroxy end groups ($\delta = 4.48$ and 5.23 ppm, respectively) and, on the other hand, the emergence of signals to the ester junction between the two blocks (i.e. two triplets at $\delta = 2.36$ and 2.33_5 ppm corresponding to the CH_2 protons in α-position of carbonyl group annoted 11″E and 11″P in the spectra, respectively, and two multiplets at $\delta = 4.27$ and 5.09 ppm relative to the CH_2 and CH protons in α-position of oxygen atom annoted 1E and 1P, respectively). Moreover, the signal at 4.48 ppm decreases more rapidly than the multiplet at 5.23 ppm which is consistent with the higher reactivity of primary hydroxy groups compared to that of secondary hydroxy groups.

3.2. Synthesis and properties of multiblock copolymers

In order to obtain block copolymers with high molar mass, the syntheses include two stages: the reaction was first carried under argon atmosphere then under vacuum. In all experiments the catalyst is Zr(OBu)$_4$ at 1.5 mmol kg^{-1} and the temperature is 240°C.

The characteristics of the block copolymers are reported in Table 3 and are compared to those of two PEBAX® samples based on polyamide-12 (PA12; $\bar{M}_n \approx 2000$) and polyoxytetramethylene (POTM; $\bar{M}_n \approx 2000$ or 1000, respectively). The abbreviated names of the different PEBAs are given in Scheme 2. The $\bar{M}_n$ and η_{inh} values relative to PEBAX® are higher than those of other multiblock copolymers. This arises from the type of the reactor which was used: an industrial one for PEBAX® and a classical laboratory reactor for the other copolycondensates.

3.2.1. Thermal behavior

3.2.1.1. Differential scanning calorimetry and thermogravimetric analysis. The thermal characteristics of PA12dC, α,ω-dihydroxy-polyethers and PEBAs are reported in Tables 4 and 5.

DSC analysis reveals the semicrystalline character of POEdOH and POTMdOH and the wholly amorphous

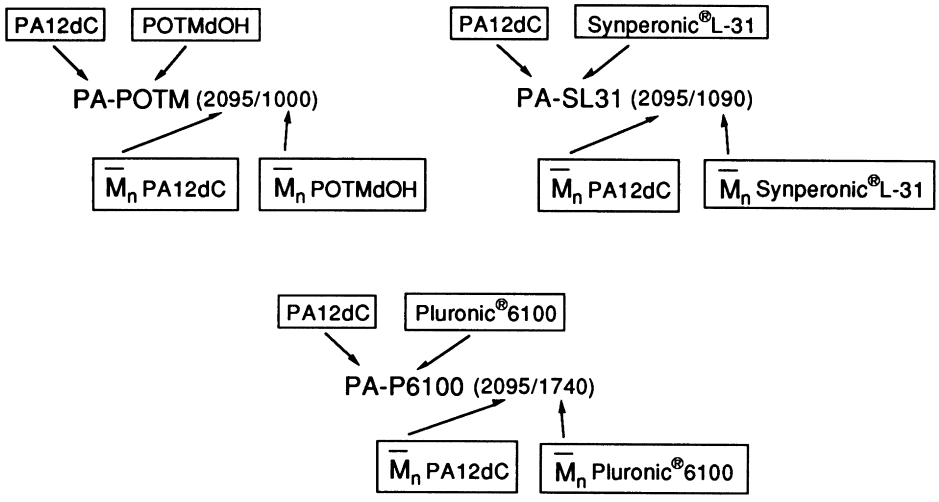

Scheme 2.

Table 4
Thermal characteristics of initial oligomers determined by DSC (in the second heating run with a rate of 20°C/min) and TGA: glass transition temperature T_g, recrystallization temperature T_c, heat of recrystallization ΔH_c, melting temperature T_m, heat of fusion ΔH_m and 10% mass loss temperature $T_{10\%}$

Sample	T_g (°C)	T_c (°C)	$-\Delta H_c$ (J g^{-1})	T_m (°C)	ΔH_m (J g^{-1})	$T_{10\%}$ (°C)
PA12dC	–			165	75	400
POTMdOH	−82			21	90	237
POEdOH	−67			39	143	267
POPdOH	−71					275
Synperonic®L-31	−71					275
Synperonic®L-35	−60	−44	35	29	40	300
Synperonic®L-42	−69	−41	15	−9	14	280
Synperonic®L-61	−69					270
Pluronic®3100	−70					250
Pluronic®4300	−68	−44	19	−4	21	315
Pluronic®6100	−69					280

character of POPdOH. In the same way, Synperonic®L-35 and L42 and Pluronic®4300 copolyethers are semicrystalline; the corresponding thermograms (Fig. 6a) exhibit a recrystallization exotherm after the glass transition. On the contrary, the Synperonic®L-61 and L-31, Pluronic®6100 and 3100 copolyethers are fully amorphous. This fact is undoubtedly due to the higher percentage of OP units contained in the copolymers of the second series (Table 1). Whatever the copolyether, the glass transition (T_g) occurs at about −70°C except Synperonic®L-35 which presents T_g at −60°C.

A glass transition at low temperature (−75 to −55°C) and a melting transition close to 165°C are observed in all PEBA thermograms. The glass transition is that of the amorphous polyether-rich phase (T_{gPE}) and the melting transition is that of the crystalline polyamide-rich phase (T_{mPA}); the latter remains practically unchanged whatever the initial oligoether and close to that of the initial oligoamide. This melting endotherm exhibits a shoulder observed at lower temperature (130–140°C) due to the presence of small and imperfect crystallites [16]. The heat of fusion ΔH_{mPA}, calculated with respect to the polyamide phase, is lower than that of initial oligoamide, but its value does not significantly change with the length and nature of polyether block.

As expected, the POP blocks are amorphous in multiblock copolymers prepared from homopolyethers. The POE and POTM blocks of $\bar{M}_n \approx 1000$ crystallize very little or not at all when they are linked to polyamide blocks. The glass transition temperatures T_{gPE} of these POP, POE and POTM blocks are always higher than those of initial homopolyethers. In particular, the transition of the soft block of the copolymers based on POTM of $\bar{M}_n \approx 1000$ (i.e. PA-POTM(2095/1000) and PEBAX®(2000/1000) samples), stretches on a very broad range of temperature (from −85 to −15°C) (Fig. 6b). These shifts (from 13 to 34°C) in the values of T_g provide some information about phase separation in materials: the soft polyether units (particularly POTM and POP) are to some extent compatible with the rigid polyamide-12 units in the amorphous phase.

The POTM block of $\bar{M}_n \approx 2000$ remains semicrystalline in PEBAX®(2000/2000) since a melting endotherm T_{mPE}

Table 5
Thermal characteristics of PEBAs determined by DSC (in the second heating run with a rate of 20°C/min) and TGA

Sample	T_{gPE} (°C)	T_{mPE} (°C)	ΔH_{mPE} (J g_{PE}^{-1})	T_{mPA} (°C)	ΔH_{mPA} (J g_{PA}^{-1})	$T_{10\%}$[c] (°C)
PEBAX®(2000/2000)	−75	9[a]	32	164	54	415
PEBAX®(2000/1000)	−54			162	54	415
PA-POTM(2095/1000)	−48			161	52	415
PA-POE(2095/1050)	−54	11[b]	10	161	55.5	415
PA-POP(2095/880)	−53			161	54	380
PA-SL31(2095/1090)	−57			162	54.5	390
PA-SL35(2095/1920)	−61			166	54	400
PA-SL42(2095/1570)	−61			162	54	395
PA-SL61(2095/1950)	−64			166	56	380
PA-P3100(2095/1095)	−56			165	50	380
PA-P4300(2095/1925)	−60			166	56	395
PA-P6100(2095/1740)	−63			163	52	395

[a] In the first heating run $T_{m1PE} = 9°C$ and $T_{m2PE} = 49°C$ with $\Delta H_{m1PE} = 8$ J g_{PE}^{-1} and $\Delta H_{m2PE} = 22$ J g_{PE}^{-1}, respectively.
[b] In the first heating run $T_{mPE} = 11°C$ with $\Delta H_{mPE} = 5$ J g_{PE}^{-1}.
[c] Ten percent mass loss temperature.

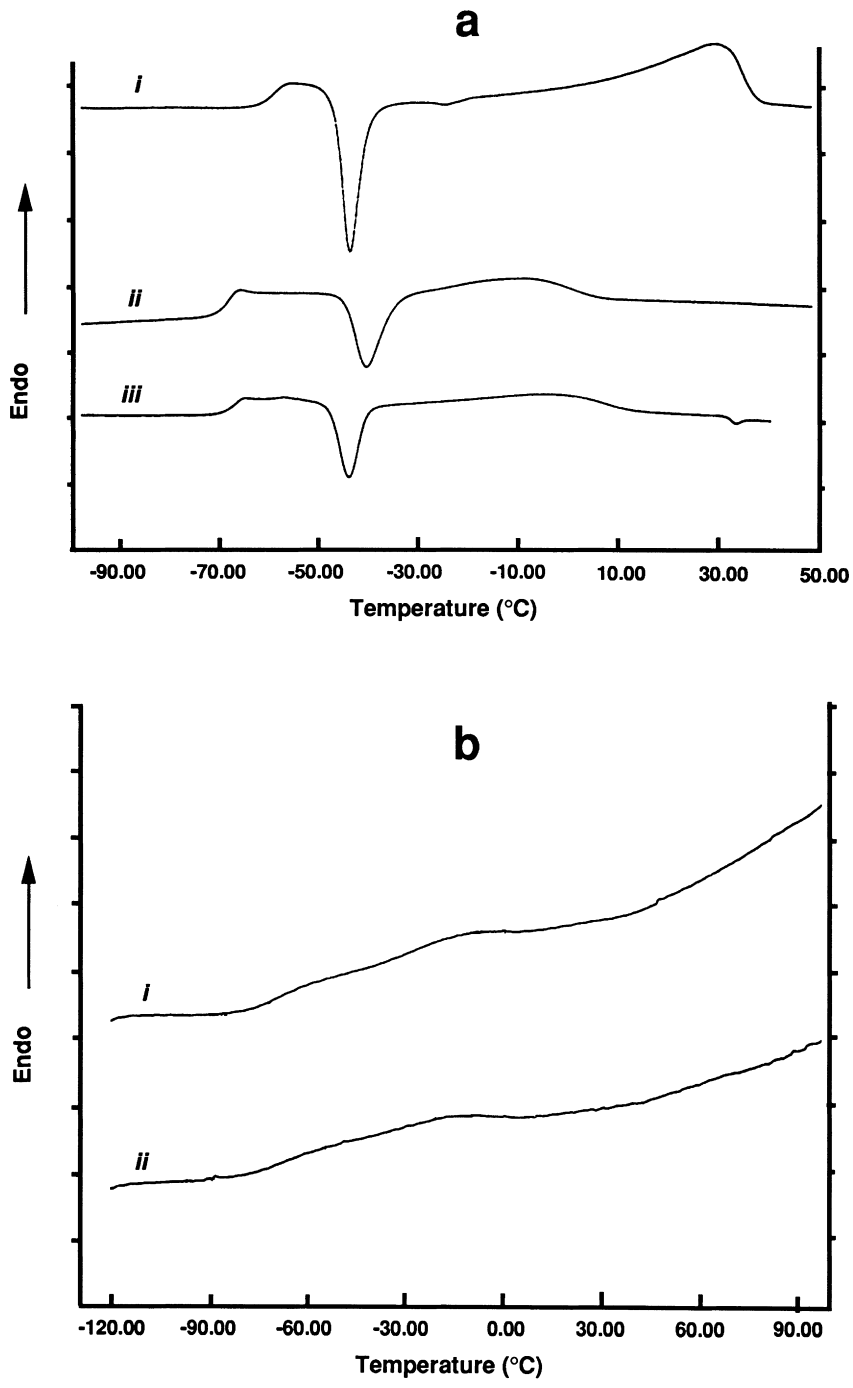

Fig. 6. DSC thermograms of (second heating run at 20°C/min): (a) copolyether precursors (i) Synperonic®L-35, (ii) Synperonic®L-42, (iii) Pluronic®4300; (b) multiblock copolymers (i) PA-POTM(2095/1000), (ii) PEBAX®(2000/1000).

appears at about 9°C with a low heat of fusion ΔH_{mPE} (~32 J/g_{PE}) compared to the value of initial POTMdOH (~94 J/g). This phenomenon has already been observed by Xie and Camberlin [9] who studied PEBAX® samples containing various lengths of PA12 and POTM blocks, respectively. In the present sample, the T_{gPE} of POTM block is only ca. 8°C higher than that of polyoxytetramethylene of $\bar{M}_n \approx 2000$ which indicates the presence of better phase separation.

The soft blocks of copolycondensates based on copolyethers do not crystallize whatever their nature and length. When the $\bar{M}_n$ of copolyether block is ca. 1000 (Synperonic®L-31 and Pluronic®3100), the corresponding T_{gPE} is only 14°C above the value of the copolyether precursor. Moreover, this shift decreases with the increasing copolyether $\bar{M}_n$ ($\Delta T \leq 8$°C). This means that these materials exhibit a high degree of phase separation.

The thermal decomposition temperature of multiblock

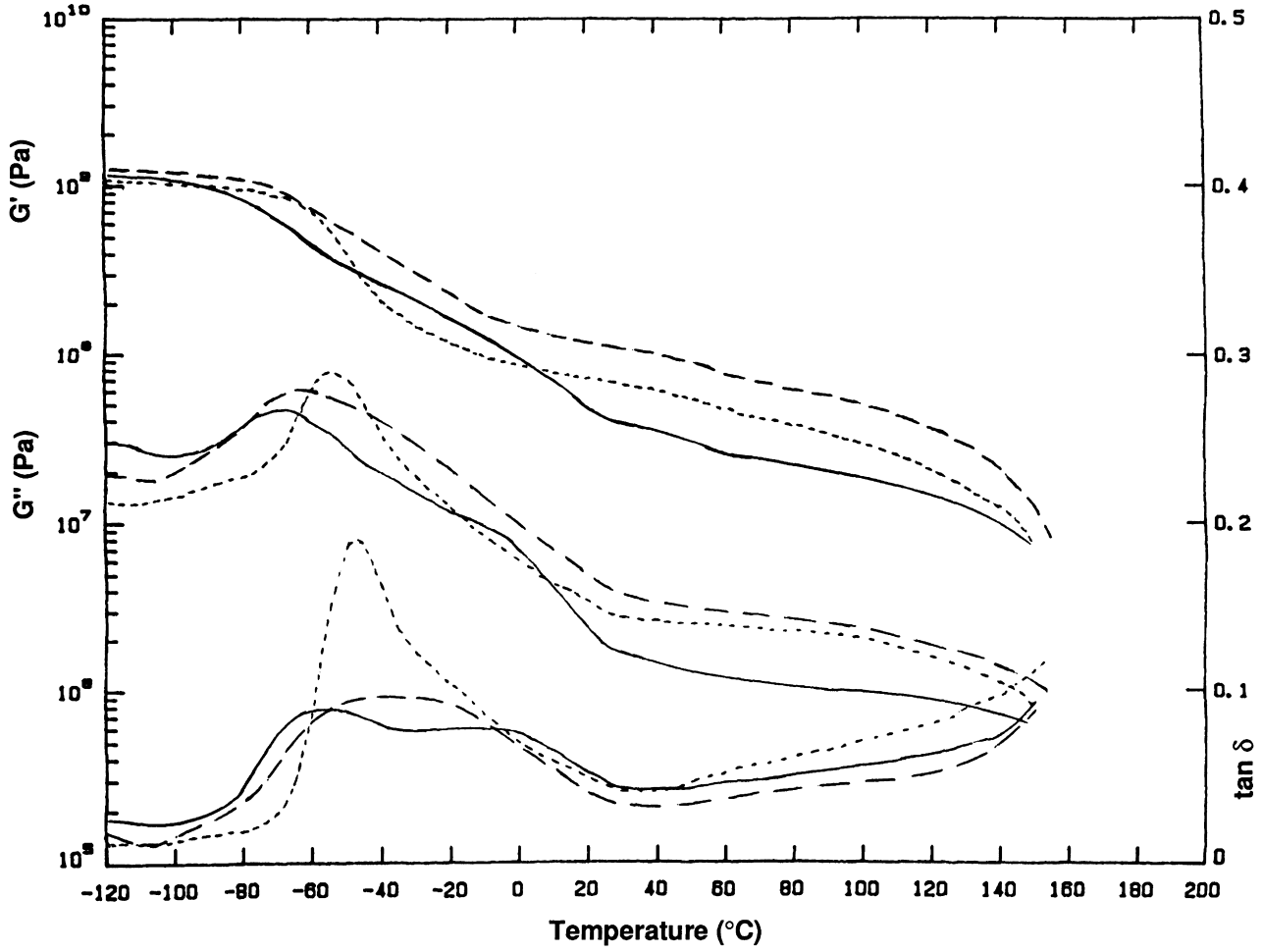

Fig. 7. Dynamic mechanical properties of: — PEBAX®(2000/2000); ––– PEBAX®(2000/1000); - - - - - - PA-POP(2095/880).

copolymers, in nitrogen atmosphere ($T_{10\%}$: 10% mass loss temperature determined by TGA analysis) takes place between 380 and 415°C; these values are close to that of oligoamide precursor ($T_{10\%} = 400$°C), although that of the polyether precursors is much lower ($237°C \leq T_{10\%} \leq 315$°C). Nevertheless, we can notice that the copolycondensates containing OP units in the soft blocks present values of $T_{10\%}$ slightly lower than those of other copolymers.

3.2.1.2. Dynamic mechanical analysis Dynamic mechanical analysis has already been applied to various PEBAs [4,9,11,17–22]. Typical dynamic viscoelastic properties of most multiblock copolymers synthesized in this work are given in Figs. 7–9. All PEBAs exhibit an important drop of storage modulus (G') between −80 and +20°C followed by a very low drop at 55–60°C. The latter corresponds to the glass transition of the hard PA12 block.

The loss modulus (G'') curve of PEBAX®(2000/1000) exhibits one peak at −60°C followed by a shoulder at about −20°C (Fig. 7). The maximum corresponds to the T_g of soft POTM segment and the relaxation at −20°C should corresponds to some glass transition between the T_gs of soft and hard blocks. Besides, the loss tangent (tan δ) curve exhibits only one very broad peak centred at −40°C. This result is in good accordance with the DSC data suggesting that part of the soft blocks are incorporated into the amorphous region of the hard domain.

The tan δ curve of PEBAX®(2000/2000) (Fig. 7) exhibits two maxima at −60 and 0°C, respectively. The first one is relative to the T_g of the POTM block and the latter principally corresponds to the melting of the POTM crystalline phase [9]. Apparently, the microphase separation of this sample seems to be more complete than that of the block copolymer based on POTM of $\bar{M}_n \approx 1000$.

The tan δ curve of PA-POP(2095/880) (Fig. 7) exhibits a maximum at −48°C, corresponding to the T_g of POP block; this peak is narrower than that of PEBAX®(2000/1000) sample, showing that the PA-POP(2095/880) copolymer presents a better phase separation.

The tan δ curves of all poly(polyamides-*block*-copolyethers) are characterized by a very narrow peak located at copolyether block T_g (Figs. 8 and 9, Table 6) and its intensity increases with soft block $\bar{M}_n$. All these copolymers exhibit a very high degree of phase separation.

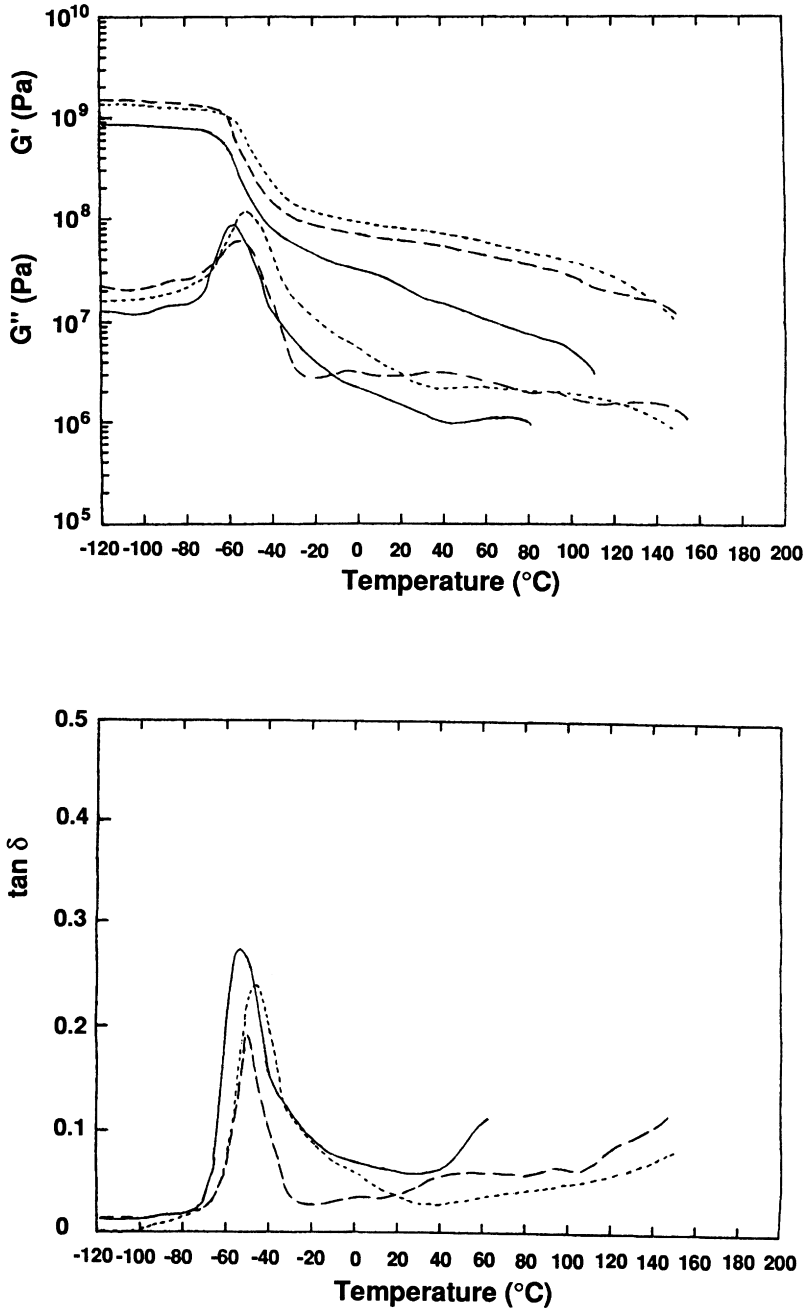

Fig. 8. Dynamic mechanical properties of: — PA-SL31(2095/1090); –– PA-P3100(2095/1095); - - - - - - PA-SL42(2095/1570).

3.2.2. Solid-state NMR analysis

The structure and morphology of PEBAs were analyzed by solid-state ^{13}C NMR. Hatfield et al. [23,24] applied this technique to two PEBAs with POE as soft blocks and polyamide-6 or polyamide-12 as rigid blocks showing that the crystalline polyamide phase of both polymers adopts a structure (α or γ) similar to that of the corresponding homopolyamide.

The ^{13}C CP/MAS NMR spectrum of PA12dC telechelic oligomer is given in Fig. 10 with the assignments of the chemical shifts. This analysis clearly indicates that the oligoamide sample crystallizes in γ-form: the trace of the spectrum and the chemical shift values are consistent with those of γ-form polyamide-12 [25]. In particular, the carbon in α-position of nitrogen atom peak at 39.4_5 ppm is characteristic of γ-form, whereas in the α-form this same carbon should appear at 42–43 ppm. Moreover, a X-ray diffraction study supports this affirmation as the corresponding pattern (not shown) exhibits two reflections with *d* spacing of 4.12 and 15.22 Å specific of γ-form which fit Ishikawa et al.'s results [26].

The ^{13}C CP/MAS NMR spectra of PEBAX®(2000/2000), PA-POTM(2095/1000), PA-POE(2095/1050) and

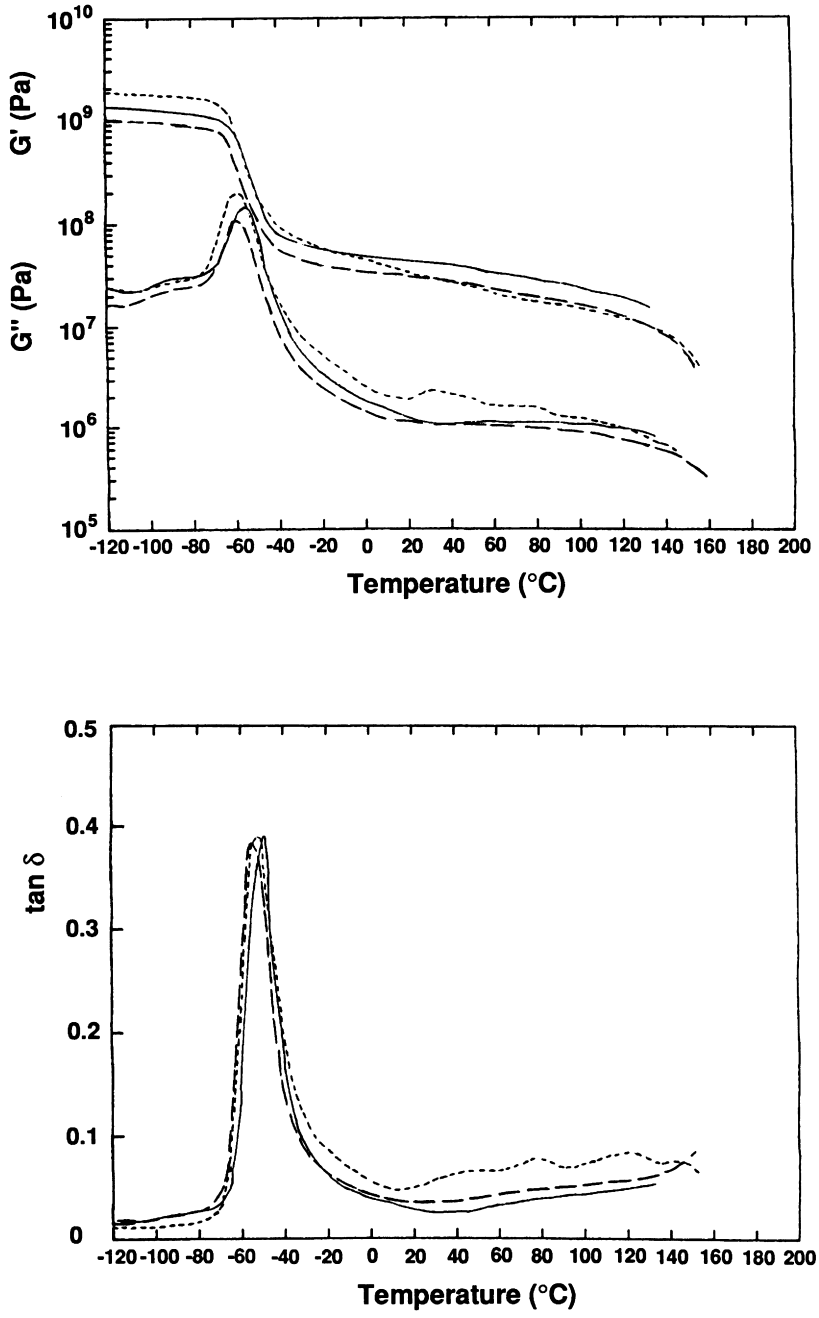

Fig. 9. Dynamic mechanical properties of: — PA-SL35(2095/1920); ––– PA-SL61(2095/1950); - - - - - - PA-P4300(2095/1925).

Table 6
Temperatures at the maximum of tan δ curves relative to poly(polyamides-*block*-copolyethers)

Sample	T tan δ_{max} (°C)
PA-SL31(2095/1090)	−47
PA-P3100(2095/1095)	−45
PA-SL42(2095/1570)	−52
PA-SL35(2095/1920)	−55
PA-SL61(2095/1950)	−55
PA-P4300(2095/1925)	−52

PA-POP(2095/880) are given in Figs. 11 and 12. They exhibit three regions located at:

(i) 17–40 ppm: polyamide methylene carbons and polyether methylene or methyl carbons in β-position of oxygen atom.
(ii) 63–76 ppm: polyether carbons in α-position of oxygen atom.
(iii) ~173 ppm: polyamide carbonyl group.

The small resonance peak at ca. 64 ppm visible on the spectra of copolymers based on POTM and POE are specific of methylene carbon in α-position of ester group. In the

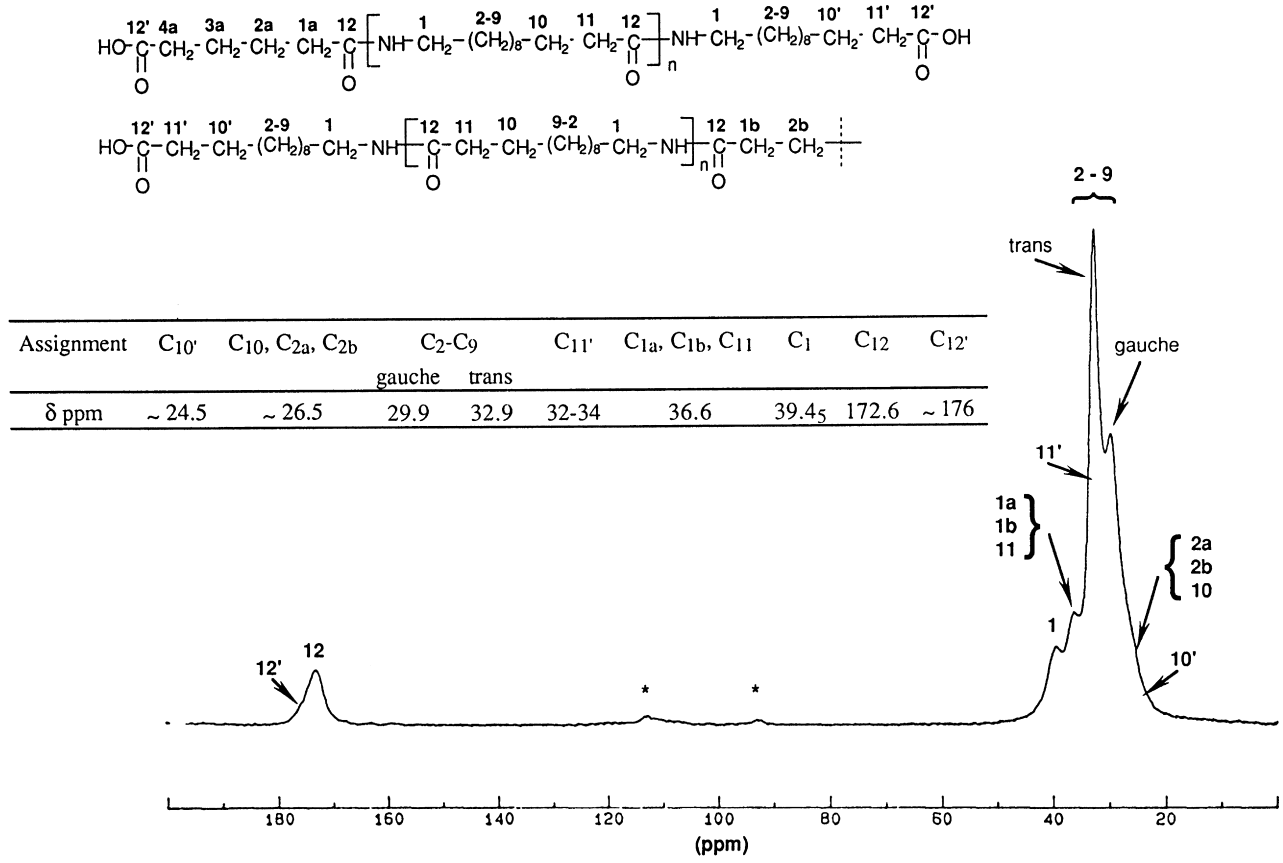

Fig. 10. ^{13}C CP/MAS spectrum of PA12dC (50.32 MHz; spinning frequency is 4 kHz; ∗: spinning sidebands).

same way, in PA/POP(2095/1000) spectrum the shoulder located at ca. 69.5 ppm corresponds to methine carbon in α-position of ester group.

In all these copolymers, the polyamide block crystalline phase is identical to that of the oligoamide precursor since the region (i) trace is consistent with the spectrum of γ-form polyamide-12.

The study of region (ii) also provides some interesting information on the structure of polyether block. The structures and morphologies of POTM, POE and POP homopolymers of high molar masses have previously been characterized by solid-state NMR [27–32]. POTM is characterized by a semi-crystalline structure as shown its ^{13}C CP/MAS NMR spectrum [27]; the latter exhibits two peaks for both types of methylene carbons in POTM: the internal methylene carbons are characterized by two peaks separated by 1 ppm, and the carbons in α-position of oxygen atom by two peaks separated by 2 ppm. In both cases, the upfield resonance corresponds to amorphous phase and the downfield one to crystalline phase. These different peaks could be easily assigned by varying the contact time of CP/MAS experiment. A very short contact time principally reveals carbons in the crystalline region; on the contrary, a long contact time reveals the amorphous ones. Consequently, ^{13}C CP/MAS NMR spectra of PEBAX®(2000/2000) were recorded using different contact times from 10 μs to 10 ms. In the range of 68–76 ppm (Fig. 13), the two peaks relative to POTM methylene carbons in α-position of oxygen atom present in the crystalline and amorphous phases are visible at 72.60 and 71.20 ppm, respectively. In the same way, the resonances of internal methylene carbons in the crystalline and amorphous phases are at 28.00 and 27.40 ppm, respectively. Moreover, the long contact time (3 ms) mainly reveals the amorphous carbons and the short contact time (30 μs) permits to clearly distinguish the crystalline and amorphous carbons, respectively. This is confirmed by the plots of $\ln(I/I_0)$ versus contact time (Fig. 14). On the other hand, whatever the contact time value, the ^{13}C CP/MAS spectrum of PA-POTM(2095/1000) (Fig. 11b) exhibits a single peak at 70.5_5 ppm showing that the POTM block of $\bar{M}_n \approx 1000$ is completely amorphous.

Dechter [28] has shown that the spectrum of high molar mass PEO, which is semicrystalline, consists of a narrow peak superimposed on a broad one at about 72 ppm; when the contact time is 100 μs, both broad and narrow peaks are observed; when the contact time is 800 μs, the narrow peak is principally observed and it corresponds to the amorphous phase of PEO whereas the broad peak is relative to the crystalline one.

The ^{13}C CP/MAS NMR spectrum of PA-POE(2095/1050) exhibits a narrow peak at 71.05 ppm even for short

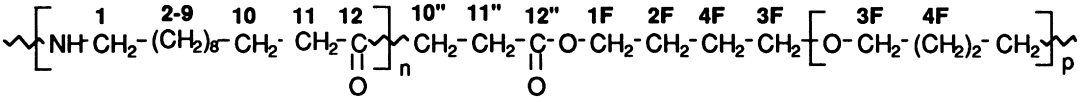

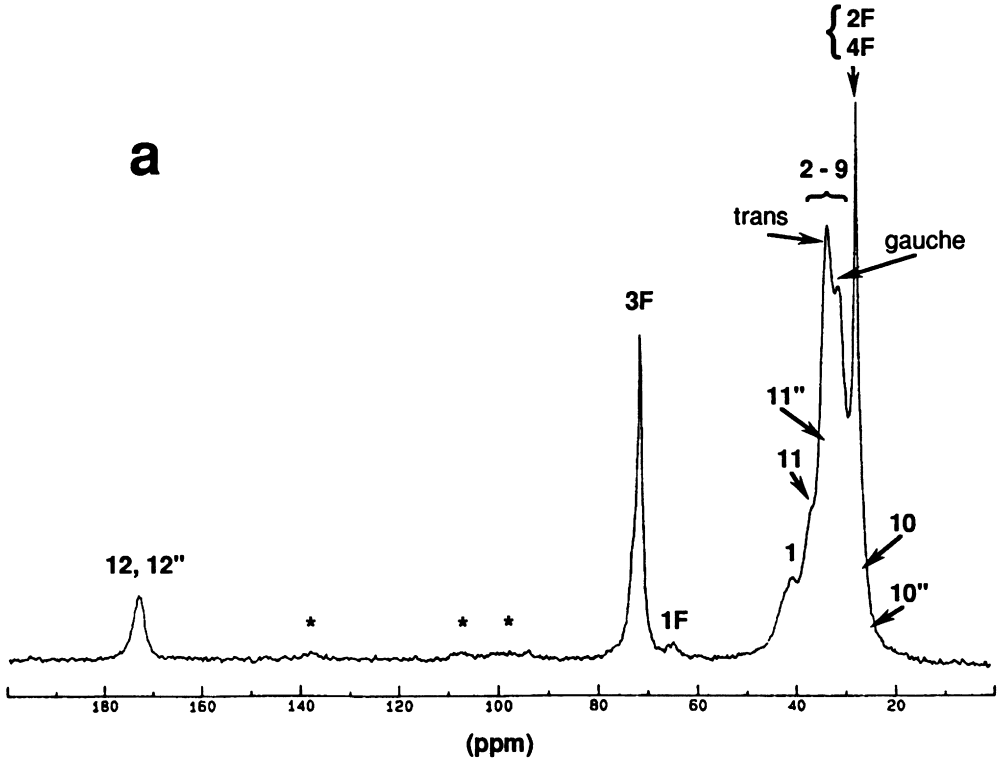

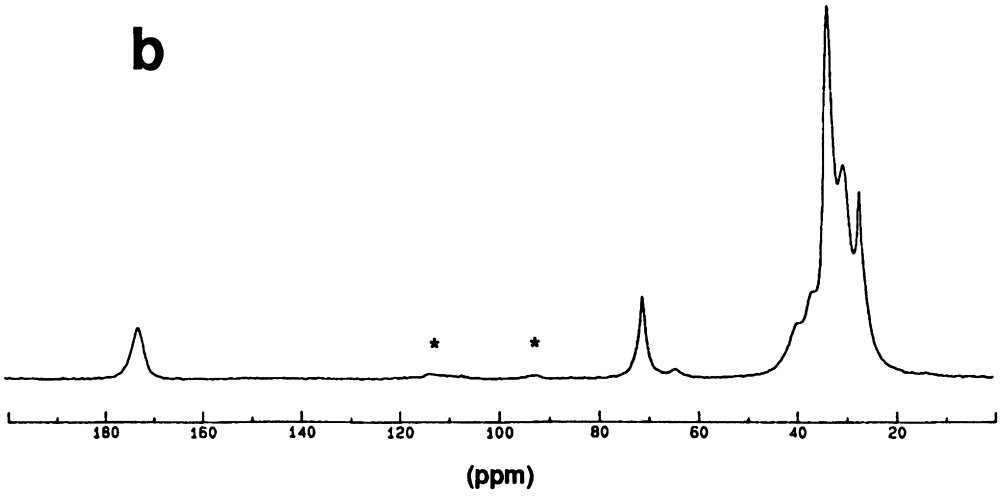

Fig. 11. ^{13}C CP/MAS spectrum of: (a) PEBAX®(2000/2000) (75.48 MHz; spinning frequency is 5 kHz; ∗: spinning sidebands); (b) PA-POTM(2095/1000) (50.32 MHz; spinning frequency is 4 kHz; ∗: spinning sidebands).

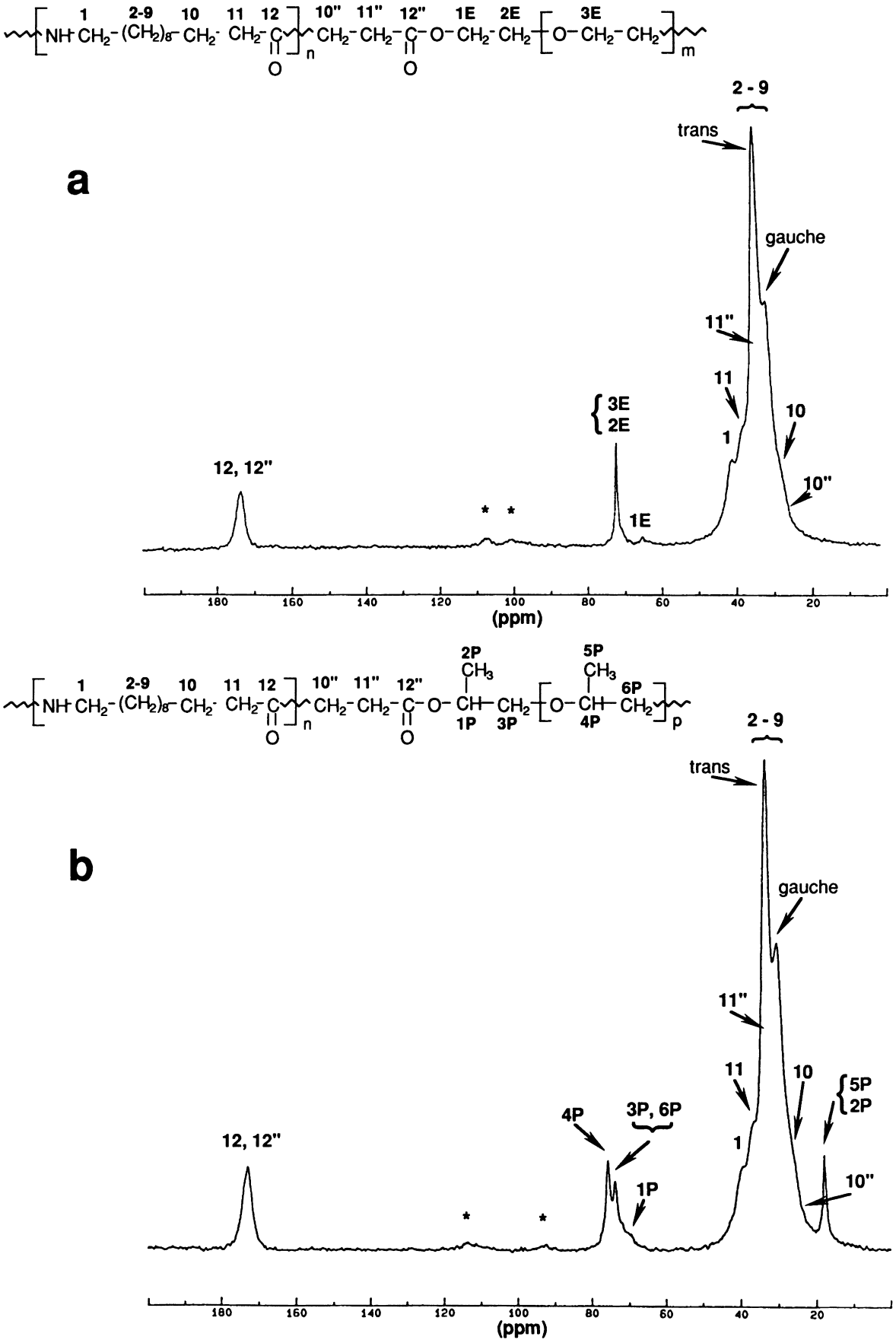

Fig. 12. ^{13}C CP/MAS spectrum of: (a) PA-POE(2095/1050) (75.48 MHz; spinning frequency is 5 kHz; ∗: spinning sidebands); (b) PA-POP(2095/880) (50.32 MHz; spinning frequency is 4 kHz; ∗: spinning sidebands).

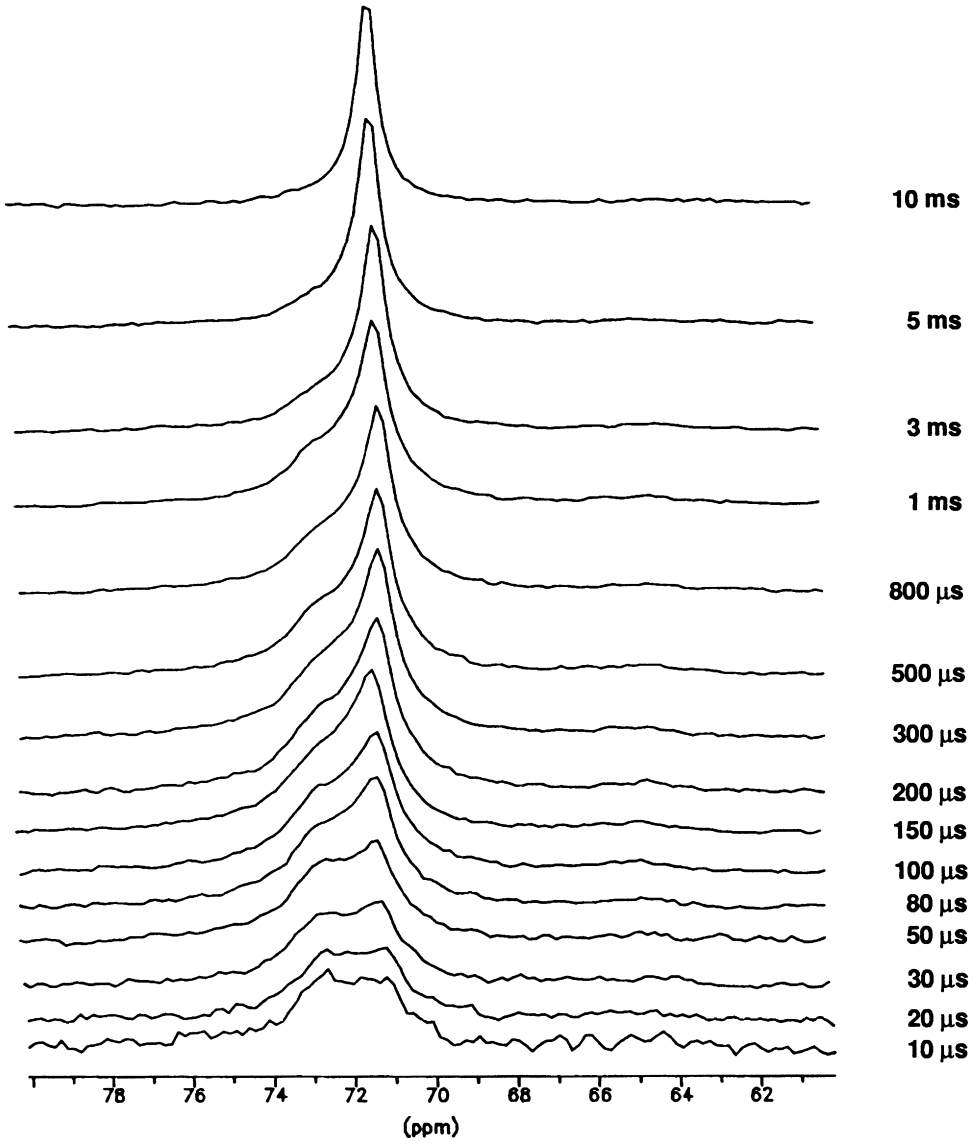

Fig. 13. ^{13}C CP/MAS spectra of PEBAX®(2000/2000) at different CP/MAS contact time (range 60–80 ppm; 75.48 MHz; spinning frequency is 5 kHz).

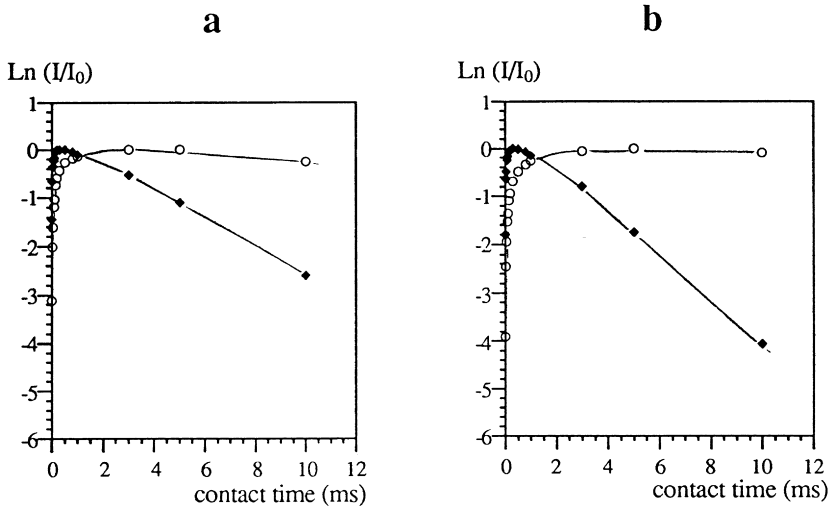

Fig. 14. Normalized CP/MAS variable contact time curves for CH_2 carbons in POTM block of PEBAX®(2000/2000): (a) in α-position of oxygen atom at: ○—71.20 ppm; ◆—72.60 ppm; (b) in β-position of oxygen atom at: ○—27.44 ppm; ◆—28.00 ppm (I symbolizes the intensity of the corresponding signal and I_0 the maximum intensity; these data were obtained from the deconvolution of spectra by computer-fitting with Gaussian and/or Lorentzian functions).

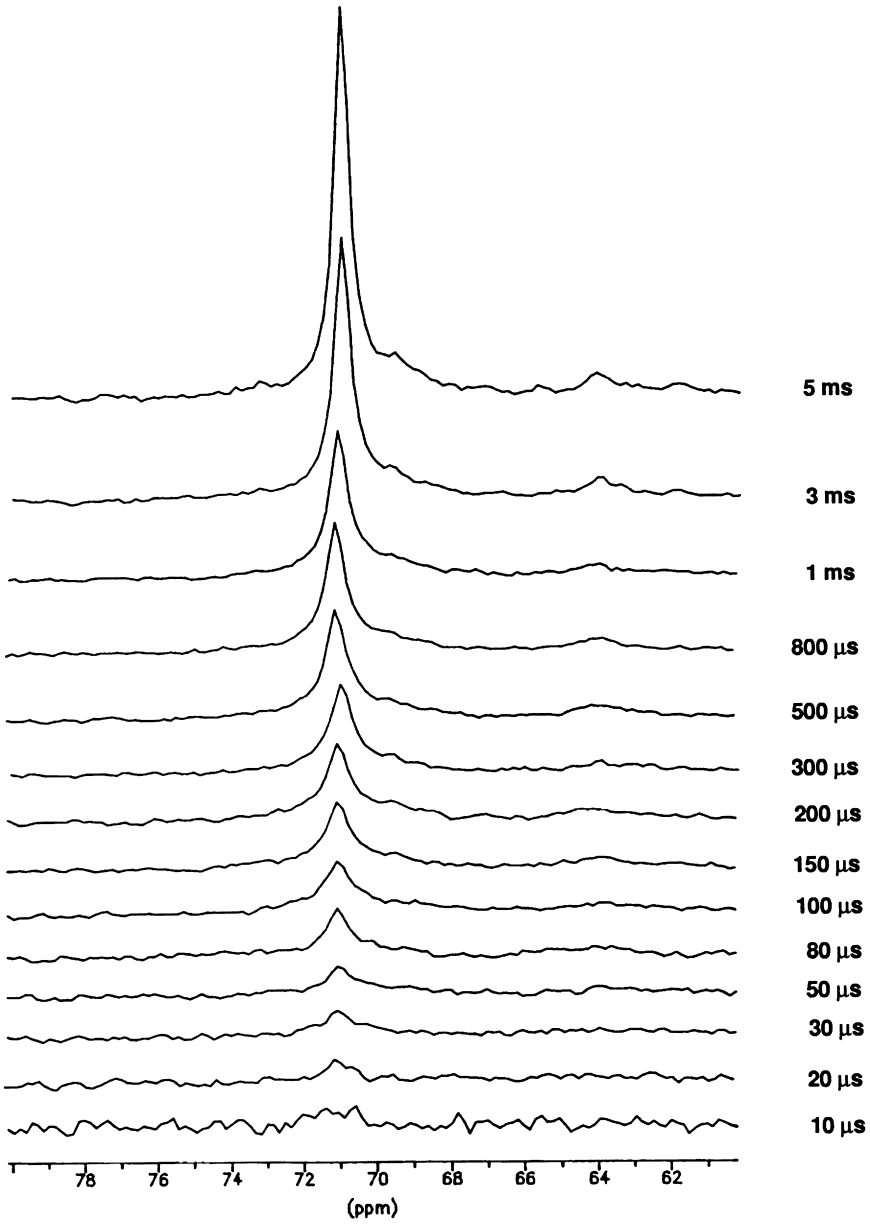

Fig. 15. ^{13}C CP/MAS spectra of PA-POE(2095/1050) at different CP contact time (range 60–80 ppm; 75.48 MHz; spinning frequency is 5 kHz).

contact times corresponding to CH_2 carbons in amorphous PEO block (Fig. 15); the DSC study has shown a weak crystallization of this block with T_{mPE} below room temperature which elucidates RMN results. Moreover, when the contact time increases, a shoulder appears at ~69.8 ppm which may correspond to CH_2 carbons present in the liquid phase of POE block.

Finally, in the ^{13}C CP/MAS NMR spectrum of PA-POP(2095/880) copolymer (Fig. 12b), three peaks characteristic of CH, CH_2 and CH_3 carbons of amorphous POP segment are observed at 75.3_5, 73.5 and 17.7 ppm, respectively. These values are in agreement with those obtained by Monnerie et al. [32] and Costa et al. [33].

The spectra of the multiblock copolymers based on Pluronic®4300 or Synperonic®L-31 copolyethers are given in Fig. 16. Whatever the length of copolyether, all the peaks characteristic of each block are observed. In particular, these spectra exhibit only one peak per carbon of the constitutive units of the soft blocks showing that these blocks are completely amorphous. In the same way, the CH_2 region of PA12 segment (25–40 ppm) shows that this block crystallizes in γ-form.

4. Conclusion

The kinetic study of the polycondensation of α,ω-dicarboxy-oligododecanamide ($\bar{M}_n = 2095$) with various α,ω-dihydroxy-polyethers ($\bar{M}_n \approx 1000 - 2000$) showed that the catalytic activity of $Zr(OBu)_4$ depends on the reactive

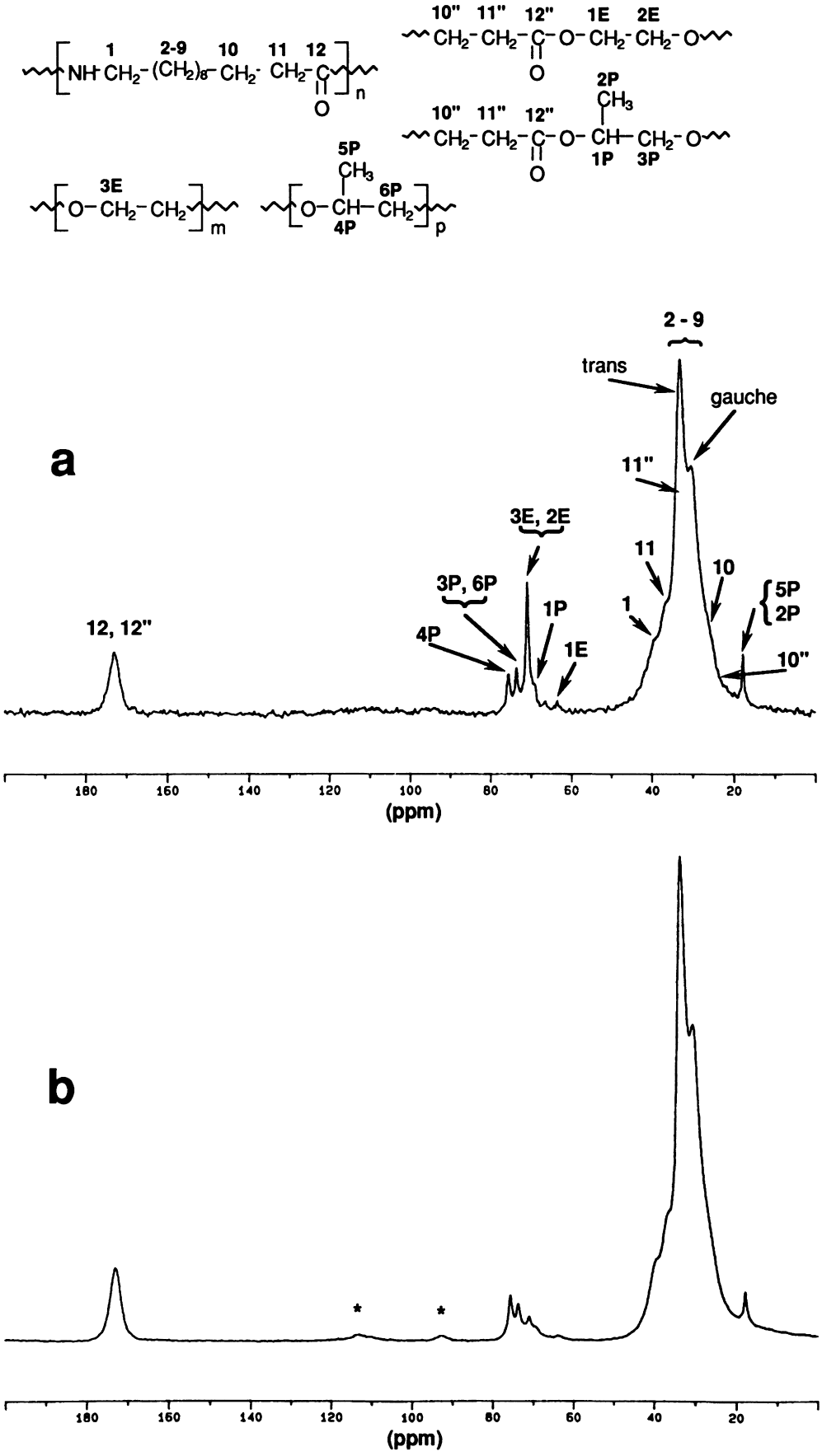

Fig. 16. ^{13}C CP/MAS spectrum of: (a) PA-P4300(2095/1925) (50.32 MHz; spinning frequency is 4 kHz; ∗: spinning sidebands); (b) PA-SL31(2095/1090) (50.32 MHz; spinning frequency is 4 kHz; ∗: spinning sidebands).

mixture. In particular, when the oxyethylene unit content and the catalyst concentation (3 mmol kg^{-1}) are high, the system exhibits an unusual behavior since the reactivity is reduced. In order to clarify this problem, we are undertaking a study dealing with the determination of the actual structure of the catalyst and of its evolution in the polyamide-polyether system. In the same way, we are looking into the behavior of other catalysts.

DSC and DMA experiments showed that the multiblock copolymers based on copolyethers containing both oxyethylene and oxypropylene units are characterized by a very high degree of phase separation; the soft copolyether blocks do not crystallize whatever their length and their composition. The use of copolyethers should lead to a new family of poly(polyethers-*block*-polyamides) with good mechanical properties between −30 and 40°C and particularly no drop of storage modulus is observed in this temperature range.

Acknowledgements

The authors thank Doctor S. Girault (Elf Atochem, Levallois Perret), Doctor C. Falce and Doctor B. Ernst (Elf Atochem, Serquigny) for X-ray diffraction, SEC, viscosimetry and DMA measurements. They also acknowledge ICI, BASF and Elf Atochem for providing Synperonic®, Pluronic® and PA12dC samples, respectively.

Alya Boulares gratefully acknowledges the “Société des Amis des Sciences” for its financial support.

References

[1] Deleens G, Foy P, Maréchal E. Eur Polym J 1977;13:337–53.
[2] Mumcu S, Burzin K, Feldmann R, Feinauer R. Angew Makromol Chem 1978;74:49.
[3] Castaldo L, Maglio G, Palumbo R. J Polym Sci Polym Lett Ed 1978;16:643.
[4] Gaymans RJ, Schwering P, de Haan JL. Polymer 1989;30:974.
[5] Van Hutten PF, Walch E, Veeken AHM, Gaymans RJ. Polymer 1990;31:524.
[6] Chung L-Z, Kou D-L, Hu AT, Tsai H-B. J Polym Sci Part A: Polym Chem 1992;30:951.
[7] Acevedo M, Fradet A. J Polym Sci Part A: Polym Chem 1993;31:1579.
[8] Yu YC, Jo WH. J Appl Polym Sci 1994;54:585.
[9] Xie M, Camberlin Y. Makromol Chem 1986;187:383.
[10] Fakirov S, Goranov K, Bosvelieva E, Du Chesne A. Makromol Chem 1992;193:2391.
[11] Yu YC, Jo WH. J Appl Polym Sci 1995;56:895.
[12] Girardon V, Correia I, Tessier M, Maréchal E. Eur Polym J 1998;34:363.
[13] Boulares A, Tessier M, Maréchal E. J Macromol Sci Pure Appl Chem 1998;A35:933.
[14] Leverd F, Fradet A, Maréchal E. Eur Polym J 1987;23:695–705.
[15] Laporte P, Fradet A, Maréchal E. J Macromol Sci Chem 1987;A24:1289.
[16] Ishikawa T, Nagai S, Kasai N. J Polym Sci Polym Phys Ed 1980;18:1413.
[17] Alberola N. J Appl Polym Sci 1988;36:787.
[18] Alberola N, Vassel A, Helluin JC. Makromol Chem Macromol Symp 1989;23:219.
[19] Sikkema DJ. J Appl Polym Sci 1991;43:877.
[20] Otsuki T, Kakimoto M-A, Imai Y. J Appl Polym Sci 1990;40:1433.
[21] Ghosh S, Khastgir D, Bhowmick AK. Polymer 1998;39:3967.
[22] Sakurai K, Amador G, Takahashi T. Polymer 1998;39:4089.
[23] Hatfield GR, Guo Y, Killinger WE, Andrejak RA, Roubicek PM. Macromolecules 1993;26:6350.
[24] Hatfield GR, Bush RW, Killinger WE, Roubicek PM. Polymer 1994;35:3943.
[25] Mathias LJ, Johnson CG. Macromolecules 1991;24:6114.
[26] Ishikawa T, Nagai S, Kasai N. J Polym Sci Polym Phys Ed 1980;18:291.
[27] Belfiore LA. Polymer 1986;27:80.
[28] Dechter JJ. J Polym Sci Polym Lett Ed 1985;23:261.
[29] Cholli AL, Schilling FC, Tonelli AE. Polym Prepr (Am Chem Soc Div Polym Chem) 1988;29:12.
[30] Zhang X, Takegoshi K, Hikichi K. Macromolecules 1992;25:2336.
[31] Zhang X, Takegoshi K, Hikichi K. Macromolecules 1993;26:2198.
[32] Dejean de la Batie R, Lauprêtre F, Monnerie L. Macromolecules 1988;21:2052.
[33] Tavares MIB, Castro WP, Costa DA. J Appl Polym Sci 1995;55:1165.